Variable-Energy Positron Lifetime Study of Silicon-Oxide Films Plasma Deposited from Hexamethyldisiloxane and Oxygen Mixtures

C. L. WANG,[1]* Y. KOBAYASHI,[1,2] H. TOGASHI,[1] K. HIRATA,[1,2] R. SUZUKI,[2] T. OHDAIRA,[2] T. MIKADO,[2] S. HISHITA[3]

[1] National Institute of Materials and Chemical Research, Tsukuba, Ibaraki 305-8565, Japan

[2] Electrotechnical Laboratory, Tsukuba, Ibaraki 305-8568, Japan

[3] National Institute for Research in Inorganic Materials, Tsukuba, Ibaraki 305-0044, Japan

Received 2 January 2000; accepted 3 March 2000

ABSTRACT: Mixtures of hexamethyldisiloxane [HMDSiO, $(CH_3)_3SiOSi(CH_3)_3$] and oxygen are plasma polymerized at different oxygen pressures (P_{O_2} = 1.3–11.4 Pa) and a fixed monomer pressure (P_m = 2.6 Pa). The discharge power is kept at 100 W throughout the work. Nanometer-size holes in the deposited films are characterized by variable-energy positron annihilation lifetime spectroscopy (PALS). Additional information on the film composition and structure is obtained by X-ray photoelectron spectroscopy and IR absorption spectroscopy. The *ortho*-positronium lifetime τ_3 and intensity I_3 increase with the P_{O_2} up to 6.2 Pa and then decrease with the P_{O_2}. PALS measurements after annealing at 400°C show that films prepared at high oxygen pressure have a less stable structure than a film deposited at a lower oxygen pressure. These results are discussed in comparison with plasma deposition of pure HMDSiO, as are the possible effects of oxygen radicals on the film structure. © 2000 John Wiley & Sons, Inc. J Appl Polym Sci 79: 974–980, 2001

Key words: plasma-polymerized film; hexamethyldisiloxane; oxygen; variable-energy positron lifetime spectroscopy

INTRODUCTION

Plasma polymer deposition or plasma-enhanced chemical vapor deposition makes it relatively easy to control the chemical composition of thin polymer films by selecting suitable deposition parameters such as the discharge power, monomer flow rate, and gas composition.[1,2] The SiO_x films plasma deposited from mixtures of an organosilicon precursor and oxygen have received much attention as candidates for low dielectric constant insulation for ultralarge-scale integrated chips[3] and high-performance gas barrier coatings for polymers.[4,5] In these applications it is important to control the chemical composition and the film structure. Low dielectric constant insulation requires a stabilized, large, open volume[3,6] whereas good gas barrier coatings require a dense structure with a minimum free volume.[4,5]

Positron annihilation lifetime spectroscopy (PALS) provides useful information on nanometer-size holes in polymers.[7–9] Some positrons injected into a polymer combine with an electron to

Correspondence to: Y. Kobayashi (kobayashi@nimc.go.jp).
* *Present address:* Center for Materials Research, Washington State University, Pullman, WA 99164-2711, USA.
Contract grant sponsors: Science and Technology Agency of Japan; Agency of Industrial Science and Technology.

Journal of Applied Polymer Science, Vol. 79, 974–980 (2001)

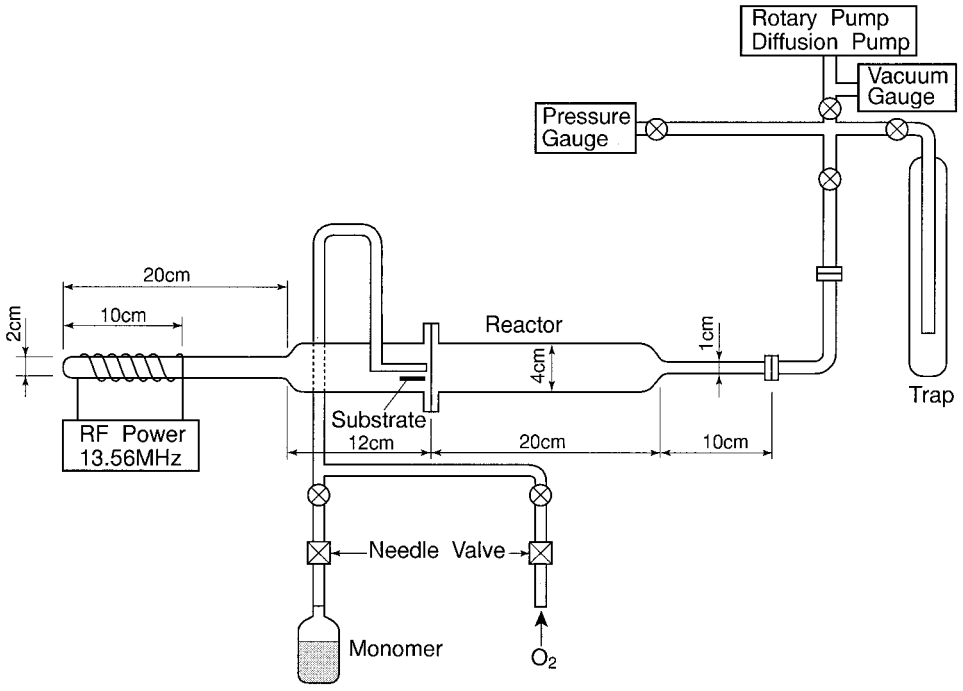

Figure 1 The plasma-enhanced chemical vapor deposition system.

form the bound state, which is positronium (Ps). The lifetime of spin-parallel *ortho*-Ps (*o*-Ps) is well correlated with the size of free volume holes whereas the *o*-Ps yield provides valuable information on the disordered structure and free radicals in a polymer.[7–9] By choosing positron energies below a few kiloelecton volts with a variable-energy pulsed beam, we probed nanometer-size holes in thin carbonized silicon-oxide films plasma polymerized from pure hexamethyldisiloxane (HMDSiO) at different monomer flow rates (F) and discharge powers (W).[10] Good correlations were observed between *o*-Ps lifetime parameters in the films and the ratio of the discharge power to the monomer flow rate (W/F).[10]

In this work, SiO_x films were plasma deposited from HMDSiO mixed with O_2 and the effect of oxygen on the free volume and structure of deposited films was studied using variable-energy PALS. Supplemental information on the chemical composition and structure was obtained by IR absorption spectroscopy and X-ray photoelectron spectroscopy (XPS).

EXPERIMENTAL

Plasma polymerization was conducted in a cylindrical glass reactor that was about 4 cm in diameter and 60 cm in length (Fig. 1).[10] After the air was removed from the HMDSiO (Tokyo Chemical Industry Ltd.) by vacuum freeze–thawing, the reactor was evacuated to a vacuum exceeding 0.01 Pa. Under steady flows of HMDSiO and oxygen, electrodeless glow discharge plasma was generated at an inductively coupled radio frequency (RF) of 13.56 MHz. Films were deposited on Si(100) substrates positioned 20 cm downstream from the discharge zone center at a constant discharge power of 100 W, a fixed HMDSiO pressure (P_m = 2.6 Pa), and different oxygen pressures (P_{O_2} = 1.3–11.4 Pa). Proper film thicknesses for IR and XPS were obtained by optimizing the deposition time (t = 1.5–3 h). Films were kept in a vacuum for at least 6 h before IR, XPS, and PALS measurements.

The IR absorption spectra of films deposited on Si wafers were recorded at room temperature with a Perkin–Elmer Spectrum-2000 with a resolution of 4 cm^{-1}. As described previously,[10] spectra were analyzed by plotting the absorption coefficient $\alpha(\omega)$ versus the radiation frequency ω after correction for coherent multiple reflections. The film thickness d and refractive index n were estimated from the period and amplitude of fringes of a baseline transmission.[11–13]

The XPS analysis was conducted with Mg Kα excitation (1253.6 eV) at a power of 280 W (VG

Table I Refractive Index (n) in IR Frequency Region and Deposition Rate (d/t) of HMDSiO Films

Film	P_{O_2} (Pa)	n	d/t (μm/h)
1	0	2.00	1.28
2	1.3	3.05	1.37
3	1.6	3.15	1.60
4	3.5	2.80	1.24
5	5.2	2.65	2.36
6	6.2	3.23	0.88
7	7.9	2.25	0.42
8	11.4	3.24	0.20

Scientific, ESCALAB 200-X with an ECLIPSE 2002 data system).[14] The atomic O/Si and C/Si ratios were estimated with Wagner's sensitivity factor.[15] To compensate for possible charging effects on peak positions,[16,17] the Si 2p peak position in each sample was calculated using the reference binding energies of C1s (284.5 eV) and O1s (531.0 eV) electrons.[18]

Positron lifetime spectra were measured using the intense pulsed positron beam at the Electrotechnical Laboratory.[19] The positron lifetimes were measured at positron energies of E = 1 and 5 keV, for which mean positron implantation depths were about 0.0040 and 0.053 mg/cm^2.[20] Lifetime spectra containing about 1 million counts were decomposed into three exponential components with the PATFIT-88 program.[21] The longest lived component with a lifetime τ_3 ranging from 3.3 to 3.9 ns and relative intensity I_3 ranging from 25 to 50% was easily attributed to the annihilation of the o-Ps localized in the nanometer-size holes.[10]

RESULTS

Deposition Rate

The film deposition rates and refractive indices in the IR frequency region deduced from IR spectra are listed in Table I. The deposition rate (d/t) first increases with increasing oxygen pressure, peaking at 2.36 μm/h at an oxygen pressure of 5.2 Pa. A further increase in oxygen pressure reduces the deposition rate to 0.20 μm/h at a P_{O_2} of 11.4 Pa.

IR Spectroscopy

Several typical FTIR spectra (raw data) for plasma films deposited at P_{O_2}/P_m = 0.5, 3.0, and 4.4 are shown in Figure 2. Even though a few are unclear, common absorption bands are observed at 1035, 840, and 810 cm^{-1}. The peak at 1035 cm^{-1} is due to Si—O—Si stretching, while the next two peaks are due to Si—$(CH_3)_3$ and Si—$(CH_3)_2$ wagging[5,10] with a small contribution from Si—O—Si stretching at 756 cm^{-1}.[22] Despite the presence of these common bands, differences occur among the three spectra. The film spectrum at P_{O_2}/P_m = 0.5 has an additional peak at 1260 cm^{-1} that is due to Si—CH_3 stretching, while this peak is extremely weak in films with P_{O_2}/P_m = 3.0 and 4.4. The relative intensities of the peaks at 840 and 756 cm^{-1} for films with P_{O_2}/P_m = 3.0 and 4.4 are much weaker than those for the film with P_{O_2}/P_m = 0.5. A band centered at 450 cm^{-1}, which is due to the rocking of the Si—O—Si bond,[23] is significantly stronger for films with P_{O_2}/P_m = 3.0 and 4.4 than for films with P_{O_2}/P_m = 0.5. An additional shoulder at 1130 cm^{-1} appears in films with P_{O_2}/P_m = 3.0 and 4.4, which possibly originates in the charge oscillation and interference between the different SiO_4 tetrahedra in the SiO network[22] or is due to the formation of a SiO_2 network with larger Si—O—Si bond angles.[6,24] According to Kirk,[23] disorder-induced mechanical coupling between transverse-optic and longitudinal-optic vibrational modes leads to the appearance of this shoulder at 1130 cm^{-1}.

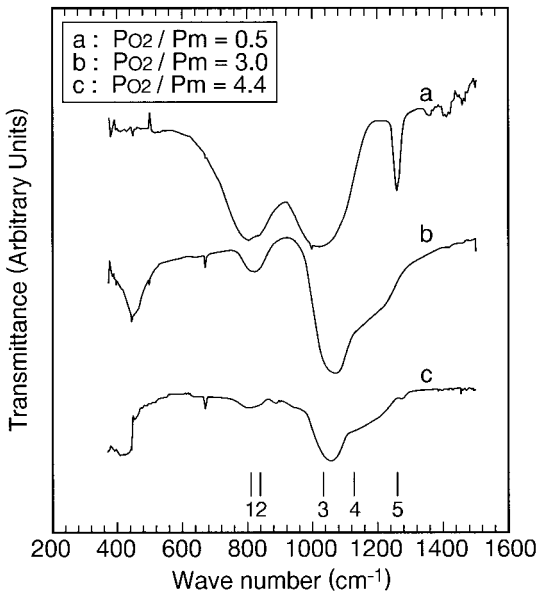

Figure 2 FTIR spectra of three films deposited at P_{O_2}/P_m ratios of 0.5 (curve a), 3.0 (curve b), and 4.4 (curve c). For easy comparison, the curves are shifted vertically. Points 1–5 are 810, 840, 1035, 1130, and 1260 cm^{-1}, respectively.

Si—O—Si bands around 920–1200 cm^{-1} are well separated from Si—$(CH_3)_3$ and Si—$(CH_3)_2$ bands. To get more quantitative information on these bands, we evaluated the following quantities as previously[10]: the integrated absorbance I of absorption peaks in $\alpha(\omega)$ via $I = \int \alpha(\omega)/\omega d\omega$[12]; peak position ω_0[25]; and the width Γ of peaks in the imaginary part of refractive index $k(\omega)$,[25] which correlates with $\alpha(\omega)$ as $\alpha(\omega) = 4\pi k(\omega)\omega$. We calculated these quantities based on least-squares analysis by approximating SiO_2 bands at 920–1200 cm^{-1} with one or two Gaussians.

Figure 3 shows variations in the integrated absorbance, width, and position of the Si—O—Si peak as a function of P_{O_2}/P_m. At $P_{O_2}/P_m = 2.4$, the peak splits into two (one peak centered at 1035 cm^{-1} and one shoulder centered around 1130 cm^{-1}), so that two values are shown in each plot for $P_{O_2}/P_m \geq 2.4$. The appearance of the shoulders indicates that the degree of disorder (or heterogeneity)[23,25] of the films prepared at $P_{O_2}/P_m \geq 2.4$ is increased in comparison with films prepared at $P_{O_2}/P_m < 2.4$. As the P_{O_2}/P_m increases, the total Si—O—Si peak intensity first increases, peaks at $P_{O_2}/P_m = 3$, and then decreases. The peak positions at 1035 and 1130 cm^{-1} shift upward with increasing P_{O_2}/P_m. The width of the peak at 1035 cm^{-1} shows a sudden change at $P_{O_2}/P_m = 2.4$.

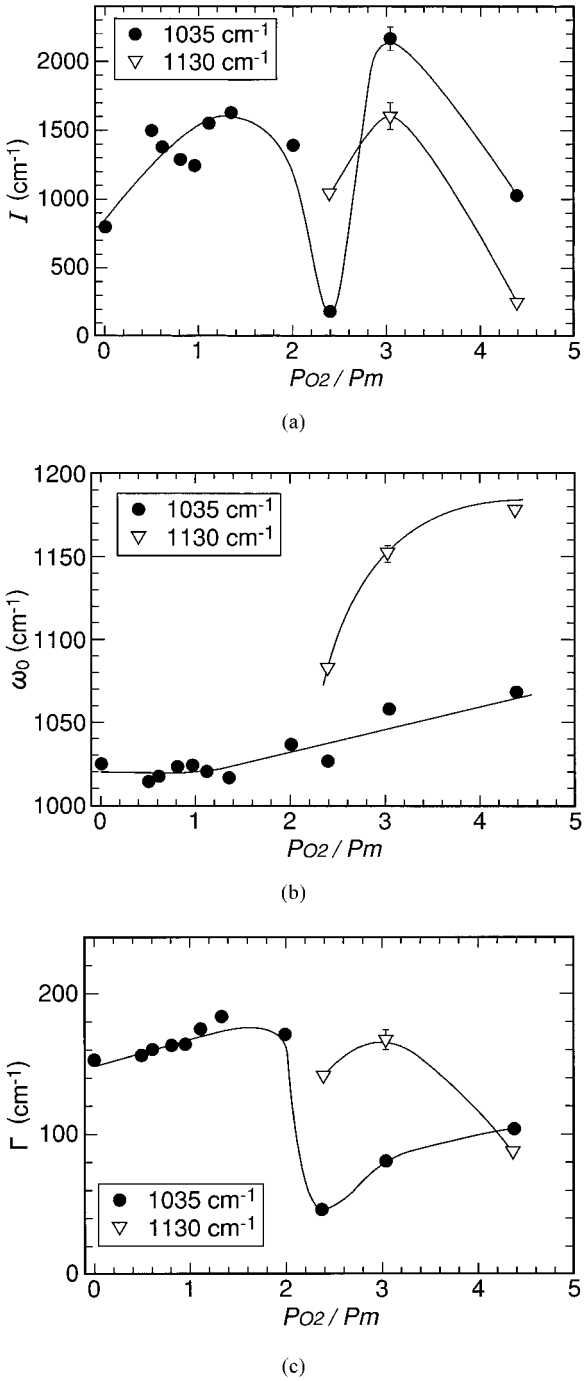

Figure 3 The effect of P_{O_2}/P_m on the IR absorption bands at 1035 and 1130 cm^{-1} (Si—O—Si): (a) integrated absorbance I , (b) central peak position ω_0, and (c) width Γ. These parameters were evaluated by approximating absorption bands as one or two Gaussians.

XPS

Information on the elemental composition and chemical state of films obtained by XPS is summarized in Figure 4. The O/Si ratio of the film deposited without oxygen is 0.8 [Fig. 4(a)]. A comparison of the value with the atomic ratio of the monomer (O/Si = 0.5) shows that oxygen atoms are incorporated during polymerization. The O/Si ratio gradually increases at the expense of the C/Si ratio with increasing P_{O_2}/P_m, indicating the elimination of methyl groups, and an increasing number of Si—O—Si bonds are incorporated at higher oxygen pressure.

Chemical shifts of photoelectron peaks result from the relaxation of the core levels of an atom after the charge is transferred to or from the valence shell because of binding with other atoms.[16,26] The variations in the binding energies (or peak positions) of the Si 2p peaks are shown in Figure 4(b). The Si 2p binding energy increases with increasing oxygen pressure. The Si 2p level is known to shift toward higher energies when Si—O bonds are formed.[26] The shift grows as the number of Si—O bonds increases, and the shift per Si—O bond is about 1 eV.[26] The results in Figure 4(b) thus suggest that concentrations of suboxides (SiO_x, x = 1, 2, 3, and 4) with higher x are enhanced with the P_{O_2}/P_m ratio.

PALS

Figure 5 shows *o*-Ps lifetimes (τ_3) and intensities (I_3) obtained by variable-energy PALS as a function of P_{O_2}/P_m. The lifetimes τ_3 are unchanged in the range of P_{O_2}/P_m between 0.5 and 1.4. They then increase and peak at $P_{O_2}/P_m = 2.4$. An empirical equation relating the *o*-Ps lifetime to the hole size was developed by Tao[27] and Eldrup et al.[28]; it is known to reproduce known hole sizes in zeolites and other molecular substances.[29] The use of the equation gives hole volumes shown on the scale at right in Figure 5(a). The cavity size was 0.23–0.30 nm^3. The *o*-Ps intensities I_3 show a behavior similar to the lifetimes; they first increase and later decrease with increasing oxygen pressure. Note that the I_3 of the film prepared at an oxygen pressure of 6.2 Pa is very high (about 48%) and close to the value for conventional poly-

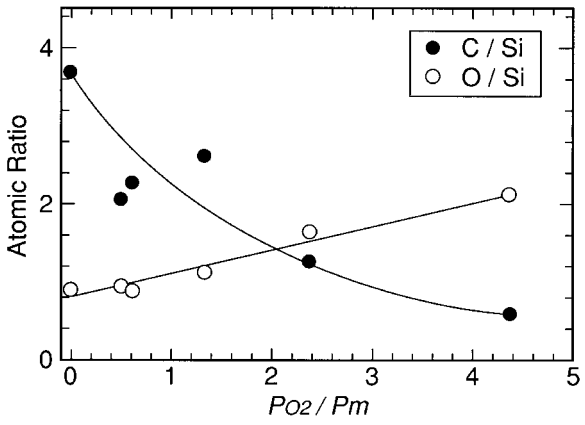

Figure 4 XPS results as a function of P_{O_2}/P_m: (a) atomic ratios C/Si and O/Si and (b) Si 2p binding energy. The values were obtained using a reference binding energy of (●) C1s (284.5 eV) and (○) O1s (531.0 eV).

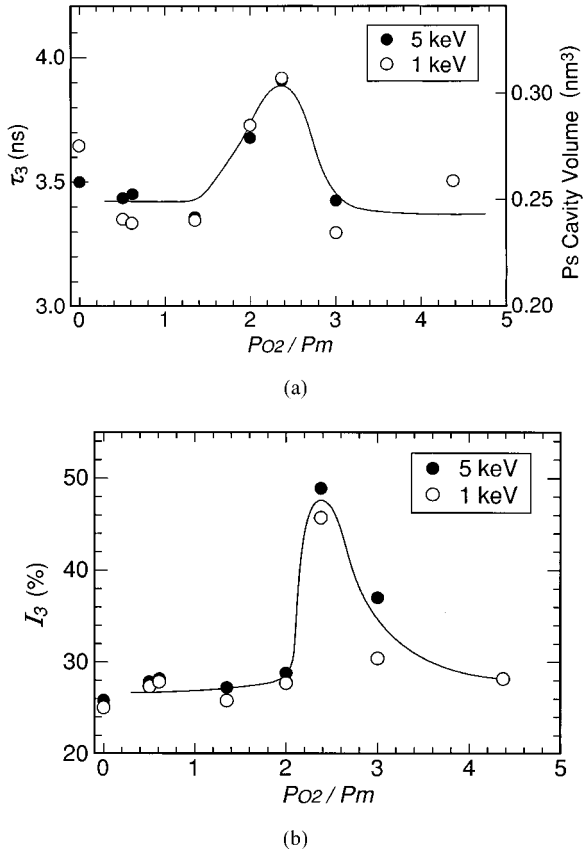

Figure 5 Variations of (a) *o*-Ps lifetimes τ_3 and (b) *o*-Ps intensities I_3 at $E = 1$ and 5 keV as a function of the pressure ratio P_{O_2}/P_m. The data are presented for as-deposited films at positron energies for (●) 5 and (○) 1 keV. Typical errors are 0.03 ns for τ_3 and 0.2% for I_3. The cavity volume was deduced as $(4\pi/3)R^3$, where R is the cavity radius given by the following equations[28]:

$$\tau_3 = 0.5 \text{ (ns)} \{1 - (R/R_0) + 0.159 \sin(2\pi R/R_0)\}^{-1}$$

$$R_0 = R + 0.166 \text{ nm}$$

(dimethylsiloxane) (44.2%)[30] and a plasma film of pure HMDSiO (47%) deposited at a high HMDSiO pressure of 4.7 Pa (at 100 W).[10]

To study the thermal stability of the deposited films, three samples were annealed in a vacuum at 400°C and PALS measurements were made at room temperature (Table II). After annealing, the τ_3 and I_3 are both significantly reduced for films 6 (P_{O_2} = 6.2 Pa) and 7 (P_{O_2} = 7.9 Pa) whereas they are essentially unchanged for film 2 (P_{O_2} = 1.3 Pa). In plasma films of pure HMDSiO a 6–10% increase in *o*-Ps yield was observed upon annealing, which was related to the disappearance of free radicals.[10] The present observation shows that structural change is more important than the disappearance of free radicals.

Table II Comparison of *o*-Ps Lifetime Parameters at $E = 5$ keV for Three HMDSiO/O_2 Plasma Films Before and After Annealing at 400°C

	Film 2 with 1.3 Pa P_{O_2}		Film 6 with 6.2 Pa P_{O_2}		Film 7 with 7.9 Pa P_{O_2}	
	As Deposited	Annealed	As Deposited	Annealed	As Deposited	Annealed
τ_3 (ns)	3.43	3.32	3.90	3.35	3.42	2.34
I_3 (%)	27.8	26.5	48.9	37.8	37.0	19.7

The error ranges are 0.01–0.03 ns for τ_3 and 0.1–0.3% for I_3. The *o*-Ps parameters at $E = 1$ keV are similar to those at $E = 5$ keV.

DISCUSSION

In contrast to plasma deposition of pure HMDSiO at a constant discharge power, where the film properties and structure systematically change as a function of HMDSiO pressure,[10,30] plasma-deposited SiO_x film from a mixture of HMDSiO/O_2 undergoes complicated structural change as a function of oxygen pressure (Figs. 2, 3, 5).

With increasing oxygen pressure in the HMDSiO/O_2 mixture, the total gas pressure increases and hence the fractional power given to HMDSiO decreases while that given to oxygen increases. (The HMDSiO pressure was kept constant in the present study.) Thus, at high oxygen pressure, because of the greater power given to oxygen, the role of oxygen radicals may become important.[31,32]

The reaction of oxygen radicals with silicon forms the Si—O bond and oxygen atoms are incorporated in the films. The reaction of oxygen radicals with carbon, however, forms volatile CO and CO_2,[33] which explains the elimination of carbon atoms and the considerable decline in the deposition rate observed at high oxygen pressures (Figs. 3, 4, Table I). At $P_{O_2}/P_m = 2.4$, the band centered around 1035 cm^{-1} in the IR spectra splits into two peaks and their peak positions progressively shift upward with increasing oxygen pressure (Fig. 3). This splitting indicates that coupling between different vibrational modes of Si—O bonds[23] is enhanced because of the increase in the vibrational degree of freedom and also the degree of disorder.[25] The onset of the new peak at 1130 cm^{-1} at an oxygen pressure of 6.2 Pa ($P_{O_2}/P_m = 2.4$) may indicate that the effect of oxygen radicals becomes significant in changing the film structure at this pressure.

The annealing data in Table II show that *o*-Ps lifetimes of films prepared at oxygen pressures of 6.2 and 7.9 Pa are significantly reduced after annealing at 400°C whereas the *o*-Ps lifetime of film deposited at $P_{O_2} = 1.3$ Pa is essentially unchanged. This indicates that films deposited at high oxygen pressure are less stable in structure than films prepared at a lower oxygen pressure. We relate the formation of such a structure at high oxygen pressure to the etching effect of oxygen radicals.[31,32] It is conceivable that in the presence of a large number of oxygen radicals the growing film is partially decomposed into fragments that may be eliminated or reorganized at a high temperature. The reduction of *o*-Ps lifetimes upon annealing suggests that the local packing density of the film probed by Ps increases. At lower oxygen pressure a more stable film may be formed from neutral HMDSiO molecules adsorbed on the surface and from the active radicals and ions mainly originating from HMDSiO without the participation of a large number of oxygen radicals.[31]

The increase of the I_3 with increasing oxygen pressure up to 6.2 Pa may be attributed to the reduction of the power given to HMDSiO. It was observed in a previous study[10] on plasma polymerization of pure HMDSiO at a constant discharge power that, because of the formation of films with less disordered structure, the I_3 systematically increases with increasing HMDSiO pressure. The introduction of oxygen to the gas phase decreases the fractional power given to HMDSiO, which may facilitate the formation of a polysiloxane-like film with high I_3 as in plasma deposition of pure HMDSiO at high pressure.

CONCLUSION

We produced thin silicon oxide films by plasma polymer deposition of HMDSiO/O_2 mixtures. The effect of oxygen on the free volume of deposited films was studied by variable-energy PALS. Ad-

ditional information on the chemical composition and network structure was obtained by XPS and IR absorption spectroscopy. We found that the oxygen concentration in the films systematically increased with increasing oxygen pressure whereas *o*-Ps lifetime parameters and IR absorption peaks due to the O—Si—O structure exhibited much more complex behavior. Films prepared at high oxygen pressure, where high concentration oxygen radicals are expected to form, were not stable after annealing at 400°C. At a lower oxygen pressure more stable film was produced. Thus, no simple correlation exists between the composition and film structure, and structural control of deposited films requires different considerations from those required for controlling the film composition. Structural information obtained by variable-energy PALS may be useful for precisely controlling the free volume and thermal stability of plasma-deposited thin films, which are important for developing such materials as gas barrier coatings and low dielectric constant insulation.

We thank Dr. K. Kato of the National Institute of Materials and Chemical Research for his help in the FTIR measurements.

REFERENCES

1. Millard, M. In Techniques and Applications of Plasma Chemistry; Hollahan, J. R., Bell, A. T., Eds.; Wiley: New York, 1974.
2. Polak, L. S., Lebedev, Y. A., Eds. Plasma Chemistry; Cambridge International Science Publishing: Cambridge, U. K., 1998; Chap. 6.
3. Grill, A.; Patel, V. J Appl Phys 1999, 85, 3314.
4. Agres, L.; Segui, Y.; Delsol, R; Raynaud, P. J Appl Polym Sci 1996, 61, 2015.
5. Inagaki, N.; Tasaka, S.; Hiramatsu, H. J Appl Polym Sci 1999, 71, 2091.
6. Han, S. M.; Aydil, E. S. J Vac Sci Technol A 1997, 15, 2893.
7. Mogensen, O. E. Positron Annihilation in Chemistry; Springer: Berlin, 1995.
8. Wang, C. L.; Hirade, T.; Maurer, F. H. J.; Eldrup, M.; Pedersen, N. J. J Chem Phys 1998, 108, 4654.
9. Ito, Y.; Kobayashi, Y. Radiat Phys Chem, to appear.
10. Wang, C. L.; Kobayashi, Y.; Togashi, H.; Kato, K.; Hirotsu, T.; Hirata, K.; Suzuki, R.; Ohdaira, T.; Mikado, T. J Appl Polym Sci 1999, 74, 2522.
11. Maley, N. Phys Rev B 1992, 46, 2078.
12. Langford, A. A.; Fleet, M. L.; Nelson, B. P.; Lanford, W. A.; Maley, N. Phys Rev B 1992, 45, 13367.
13. Manfredotti, C.; Fizzotti, F.; Boero, M.; Pastorino, P.; Polesello, P.; Vittone, E. Phys Rev B 1994, 50, 18046.
14. Hishita, S.; Oyoshi, K.; Suehara, S.; Aizawa, T. Nucl Instrum Methods Phys Res B 1999, 148, 594.
15. Wagner, C. D.; Davis, L. E.; Zeller, M. V.; Taylor, J. A.; Raymond, R. M.; Gale, L. H. Surface Interface Anal 1981, 3, 211.
16. Wucher, A. Mater Sci Forum 1998, 287, 61.
17. Gengenbach, T. R.; Griesser, H. J. Polymer 1999, 40, 5079.
18. Chastain, J., King, R. C., Jr., Eds. Handbook of X-Ray Photoelectron Spectroscopy; Physical Electronics Inc.: Eden Prairie, MN, 1995.
19. Suzuki, R.; Kobayashi, Y.; Mikado, T.; Ohgaki, H.; Chiwaki, M.; Yamasaki, T. Hyperfine Int 1994, 84, 345.
20. Vehanen, A.; Saarinen, K.; Hautojarvi, P.; Huomo, H. Phys Rev B 1987, 35, 4606.
21. Kirkegaard, P.; Pedersen, N. J.; Eldrup, M. PATFIT-88; Risoe National Laboratory: Roskilde, Denmark, 1989.
22. Wilson, M.; Madden, P. A.; Hemmati, M.; Angell, C. A. Phys Rev Lett 1996, 77, 4023.
23. Kirk, C. T. Phys Rev B 1988, 38, 1255.
24. Panov, V.; Alonso, J. C.; Ortiz, A. J Appl Phys 1999, 86, 275.
25. Ossikovski, R.; Drévillon, B. Phys Rev B 1996, 54, 10530.
26. Bell, F. G.; Ley, L. Phys Rev B 1988, 37, 8383.
27. Tao, S. J. J Chem Phys 1972, 56, 5499.
28. Eldrup, M.; Lightbody, D.; Sherwood, J. N. Chem Phys 1981, 63, 51.
29. Nakanishi, H.; Wang, S. J.; Jean, Y. C. In International Symposium on Positron Annihilation Studies of Fluids; Sharma, S. C., Ed.; World Scientific: Singapore, 1987.
30. Wästlund, C.; Maurer, F. H. J. Nucl Instrum Methods Phys Res B 1996, 117, 467.
31. Chang, C. P.; Pai, C. S.; Hsieh, J. J. J Appl Phys 1990, 67, 2119.
32. Raupp, G. B.; Cale, T. S.; Hey, H. P. W. J Vac Sci Technol B 1992, 10, 37.
33. Park, S. Y.; Kim, N. J Appl Polym Sci Appl Polym Symp 1990, 46, 91.